

Spatial-Aware Efficient Projector for MLLMs via Multi-Layer Feature Aggregation

Shun Qian¹, Bingquan Liu¹, Chengjie Sun¹
Zhen Xu¹, Baoxun Wang²

¹Harbin Institute of Technology, Harbin, China

²Tencent PCG

Abstract

The projector plays a crucial role in multimodal language models (MLLMs). The number of visual tokens it outputs affects the efficiency of the MLLM, while the quality of the visual tokens influences the visual understanding capabilities of the MLLM. Current explorations on the projector focus on reducing the number of visual tokens to improve efficiency, often overlooking the inherent spatial discrepancy between the serialized 2-dimensional visual token sequences and natural language token sequences. A **Spatial-Aware Efficient Projector (SAEP)** is proposed to address this issue. In detail, our SAEP method employs a modified separable depthwise convolution module on multi-layer visual features to enhance the spatial information of visual tokens. As a result, our SAEP method can not only largely reduce the number of visual tokens by 75%, but also significantly improve the multimodal spatial understanding capability of MLLMs. Moreover, compared to existing projectors, our SAEP gets best performances on massive multimodal evaluation benchmarks, which denotes its effectiveness on bridging the modality gap.

1 Introduction

Large Language Models (LLMs) (Chen et al., 2022; Achiam et al., 2023; Touvron et al., 2023; Chiang et al., 2023; Yang et al., 2024; Jiang et al., 2024) have demonstrated marvelous language understanding and reasoning capabilities, making a great impact on the entire AI community. Meanwhile, many vision foundation models (Radford et al., 2021; Oquab et al., 2023; Bai et al., 2024) aim to produce general-purpose visual features, which work out of the box on any vision task. As a result, multimodal works (Liu et al., 2023b; Li et al., 2023b; Liu et al., 2024; Li et al., 2024d; Dong et al., 2024a) introduce a projector to map the visual features into the token embedding space of the LLMs so that the pre-trained knowl-

edge and abilities of both LLMs and vision models can be leveraged. Multimodal Large Language Models (MLLMs) developed by such a simple technique show powerful visual instruction-following capabilities and largely raise the performance bar of various vision-language tasks.

Apparently, that the projector plays a crucial role in bridging the modality gap. It needs to convert the visual features into an ordered visual token sequence so that the visual features can be understood by LLMs (Cha et al., 2024). The number of visual tokens directly affects the computational efficiency of the MLLMs, while the quality of visual tokens affects the visual understanding capability of MLLMs. Despite the importance of the projector, there are few in-depth explorations of it.

As one of the most popular projectors, the two-layer MLP outputs the visual token sequence through the linear transformation. The MLP projector performs well in MLLMs (Liu et al., 2023b, 2024, 2023a) because the one-to-one transformation excels at preserving all local contexts of visual features. Nonetheless, there are two drawbacks in MLP projector that cannot be ignored. The first one is that MLP projector cannot control the number of visual tokens, thereby affecting the computational efficiency of MLLMs. This drawback has become much more prominent recently because a group of works (Liu et al., 2024; Dong et al., 2024b; Li et al., 2024d, 2023a) has found that the MLLMs can benefit from scaling up the resolution of input images. Unfortunately, if the resolution of the input image is doubled, there will be a sixteen-fold increase in time complexity and an inevitable explosion in memory requirements in MLLMs. The second one is that the MLP projector cannot capture spatial knowledge implicated in visual features for LLMs. In detail, the visual encoder (Radford et al., 2021; Dosovitskiy, 2020; Oquab et al.) splits and serializes the input image into a group of patch-level visual features in raster order, which is differ-

Method	#Token	S-Avg.	Ref.-Avg	VQAv2	MMB
MLP	576	46.7	51.7	78.5	64.3
SoTA	144	46.8 (Li et al., 2024b)	57.6 (Chu et al., 2024a)	78.1 (Li et al., 2024b)	66.4 (Chu et al., 2024a)
SAEP (Ours)	144	51.4	61.4	78.5	66.3

Table 1: Results of the MLP projector, state-of-the-art efficient projector and ours. They are pre-trained with the same LLaVA-1.5 training recipe for a fair comparison. “S-Avg.” refers to the normalized average score on 7 multimodal spatial tasks. “Ref.-Avg” refers to the average score on the visual grounding task over the RefCOCO+/g datasets.

ent from the left-to-right order of natural language. The simple linear transformation of MLP projector cannot alleviate this spatial and positional discrepancy and limits the performance of MLLMs. Some projectors (Jaegle et al., 2021; Li et al., 2023b; Cha et al., 2024; Chu et al., 2024a; Li et al., 2024b) are proposed to reduce the number of visual tokens, while the second problem is usually ignored. As a result, even though these works can reduce the vision token number by 75% \sim 90%, their performance is limited and is usually worse than the MLP projector.

Therefore, we propose a **Spatial-Aware Efficient Projector**, relying on multi-level features, named SAEP. It can not only largely reduce the number of visual token but also significantly improve the visual spatial understanding capabilities of MLLMs, as shown in Table 1. The performance on the general multimodal benchmarks are also improved. To be specific, the SAEP projector first reorganizes the patch-level visual feature sequence into a group of 2D “feature maps” according to their original positions. Multi-level visual features are also introduced to provide more detailed local fine grained visual cues and enhance the feature diversity without extra computational overhead. A modified depth-wise separable convolution operation is then applied on these feature maps to compress the local multiple features into a compact one, thereby enabling the preservation of spatial knowledge.

Massive multimodal evaluation benchmarks are utilized to investigate the effectiveness of our SAEP projector from different aspects. The results indicate that our SAEP projector can not only improve the computational efficiency by reduce 75% \sim 89% visual tokens, but also demonstrate extraordinary spatial understanding capability. Moreover, our SAEP projector achieves state-of-the-art performance against existing efficient projectors on the general multimodal benchmarks.

2 Related Works

2.1 Multimodal Large Language Models

Inspired by the great language understanding capabilities exhibited by Large Language Models (LLMs), the multimodal researchers take pre-trained LLMs as the pivot for information understanding and reasoning, and empower LLMs with multimodal perception capabilities to “feel” the real world and perform various multimodal tasks (Li et al., 2023b; Liu et al., 2023b,a). The pioneer works such as Flamingo (Alayrac et al., 2022) and BLIP2 (Li et al., 2023b), focus on bridge the modality gap between the pre-trained unimodal models with massive image-text pairs. LLaVA (Liu et al., 2023b) first attempts to endow the MLLMs with the ability to visual instruction-following by tuning the model with multimodal instruction-following data samples. Many subsequent works improve the MLLMs from different perspectives. Monkey (Li et al., 2024d), OtterHD (Li et al., 2023a), LLaVA-NeXT (Liu et al., 2024), InternLM-XComposer2-4KHD (Dong et al., 2024b) take high-resolution images as visual input and get noticeable performance improvement. InternLM-XComposer series (Zhang et al., 2023; Dong et al., 2024a,b), LLaVA-NeXT-Interleave (Li et al., 2024a) and Chameleon (Team, 2024) focus on generate interleaved image-text contents. Mini-Genimi (Li et al., 2024c), SPHINX-X (Gao et al., 2024), Prismatic-VLM (Karamcheti et al., 2024) employs multiple different vision encoders to capture diverse visual representations.

2.2 Vision-Language Projector

To align the visual representation space learned by the visual encoder (e.g., CLIP (Radford et al., 2021) and DINOv2 (Oquab et al.)) with the language representation space of the LLMs, different projection modules are proposed and optimized with well-designed training recipes. Resampler (Jaegle et al., 2021) and Q-former (Li et al., 2023b)

use a group of learnable query vectors to extract the textual-aligned visual embedding by the cross-attention mechanism, independent of input image resolution. Different from these elaborate projector, LLaVA (Liu et al., 2023b,a) series only use the linear MLP as the projector and gets better performance. For the purpose of improving the efficiency of MLLMs, reducing the number of visual tokens is a effectual way and a group of methods proposed. PruMerge (Shang et al., 2024) directly prunes unimportant visual tokens guided by the attention scores of the visual encoder, and merges these tokens with similarity scores. M^3 (Cai et al., 2024) aims to learn a MLLM which can capture information from mutli-granularity, variable-length visual token sequences, so that the computational cost of it can be controlled. C-Abstractor (Cha et al., 2024) adopts the Residual Blocks and average pooling layer to preserve the local context from visual features. LDPv2 (Chu et al., 2024b) takes both the point-wise and the depth-wise convolution layers for the purpose of positional information enhancement. Tokenpacker (Li et al., 2024b) introduces a region-to-point injection module to inject the fine-grained region features into the point queries, which reduces the number of visual tokens as a result. Our SAEP projector adopts the convolution layer to simultaneously serve the function of spatial understanding enhancement and token reduction.

3 Approach

3.1 Preliminary Discussion

MLLMs are developed to process multimodal inputs following the instructions and generate reasonable responses. A typically MLLM consist of three comments: a visual encoder E_v , a vision-language projector P and a LLM Φ . Firstly, the visual encoder (e.g. CLIP (Radford et al., 2021), DINOv2 (Oquab et al.)) takes the image $I_{img} \in \mathbb{R}^{3 \times H \times W}$ as input and outputs a patch-level visual feature sequence $I_v \in \mathbb{R}^{N \times C}$, where N is the number of visual features and C is the size of each visual feature. Then, the projector projects the captured visual features I_v into the token embedding space E_t modeled by the LLM. So that the LLM can understand and reason the visual information as the same way as the textual sequence T , and then generate the response $Y = \{r_i\}_{i=1}^{|Y|}$ in an autoregressive manner. The above process can be

formalized as:

$$p_{\Phi}(Y|T_v, T_t) = \prod_{i=1}^{|Y|} p_{\Phi}(y_i | y_{<i}, T_v, T_t) \quad (1)$$

where $T_v = P(E_v(I_{img}))$ and $T_t = E_t(T)$.

Due to the dominant parameter of LLM, it is primarily responsible for the majority of the computation and memory usage for MLLM. Taking the quadratic relationship between the computational expense of LLM and the number of input tokens into consideration, reducing the number of visual tokens becomes a reasonable and effective for improving the efficiency of MLLM. In addition, the projector is tasked with bridging the modality gap between the two-dimensional spatial visual signal and the one-dimensional sequential textual signal. Thus, the effectiveness of the projector significantly impacts the performance and efficiency of MLLM.

3.2 Multi-level based Spatial-aware Efficient Projector

Since the MLP projector could neither control the number of visual tokens nor capture the visual spatial knowledge from the visual features, we propose a multi-level spatial and locality-enhanced efficient projector, named SAEP, to alleviate these two problems.

Prior works (Li et al., 2022; Jiang et al., 2023a) have revealed that different layers of ViT-based model exhibit varying bias towards local and global patterns. The visual features extracted from shallower layers contain low-level local fine-grained information, while the deep layer features are superior at provide global high-level information. Hence, our SAEP projector takes multi-level visual features as its input so that more detailed and positional visual clues can be provided to the LLMs. Specifically, K layers of visual features, $\{I_v^1, I_v^2, \dots, I_v^K\}$, $I_v^k \in \mathbb{R}^{N \times C}$, are selected from the visual encoder, incurring no additional computational overhead compared to those single-layer projectors.

To facilitate the spatial structure implicated in these serialized visual features, we explicitly introduce the spatial inductive bias by converting each visual feature sequence into a group of 2D patch-grid feature maps. Formally, the same-layer visual features I_v^K are reorganized by their original relative position in the image, C feature maps is obtained, marked as $\hat{I}_v^k \in \mathbb{R}^{H \times W \times C}$, where H and W is the height and width of each feature map, and

$H \times W = N$. So there are $C \cdot K$ feature maps in total, marked as $\hat{I}_v \in \mathbb{R}^{H \times W \times CK}$.

On the basis of these feature maps, the convolution operation is applied because of its inherently advantage in preserving the spatial and positional knowledge. Instead of the standard convolution, the depthwise separable convolution is adopted so that the number of parameters and the computational complexity can be reduced. In detail, the pointwise convolution is first applied to vertically aggregate the visual features from the same position but at different levels into a more compact one. Then the depth-wise convolution operation takes in charge of horizontally aggregate the spatial regional visual features into a information enriched one. It should be noted that the stride of depthwise convolution is set the same as the kernel size to effectively reduce redundant visual information and the size of feature maps. Applying convolution uniformly across the feature map is also able to minimize information loss caused by uneven down-sampling. Moreover, an average pooling layer is also applied on the top of the pointwise convolution for regional feature compression, and its output is added to the output of depth-wise convolution operation. In essence, the average pooling layer can be seen as a simplified variant of depthwise convolution and acts as a residual-like visual feature shortcut to avoid the information loss. After the above convolution operation, the feature maps are flatten into a shorter visual token sequence.

4 Experiments

In this section, massive experiments are conducted to demonstrate the effectiveness of the proposed SAEP projector. The implementation details of the SAEP projector and the training recipe of the MLLMs are firstly described for reproduction. For the purpose of evaluation, both the vision-language spatial tasks and the popular general multimodal benchmarks (e.g., VQAv2, MME, MMBench) are selected.

4.1 Baselines

Due to most of existing vision-language projectors are designed and applied in different MLLMs with different training strategies, four most popular projectors are selected and equally employed with the training recipe of LLaVA-1.5 for a fair comparison.

¹Most results of MLP (LLaVA-1.5) are officially reported, some missed metrics are evaluated by ourselves with the officially released model checkpoint.

- **Resampler** is the most popular token reduction method. It can produce a pre-set fixed number of visual tokens with the cross-attention mechanism.
- **C-Abstractor** aims to get a balance between the efficiency and performance. The convolution and average pooling operations are introduced in it for locality modeling.
- **LDPv2** utilizes the average pooling layer for compressing the number of visual tokens and introduces a PEG module to enhance positional information.
- **Tokenpacker** injects multiple high-resolution, multi-level visual features into a coarse low-resolution one with a region-to-point attention layer. The official released LLaVA-1.5-tokenpacker checkpoint is used for evaluation because it shares the same training recipe with LLaVA-1.5 ².

4.2 Implementation Details

The SAEP projector and all the baselines are optimized with the same training recipe as the LLaVA-1.5. In detail, we take CLIP-ViT-L-336px as the visual encoder and Vicuna-7B as the LLM. Visual features from the 10th, 14th, 18th, 21st and 23rd layers of CLIP are utilized in the SAEP projector. Two-stage pre-training pipeline is adopted to get the instruction-following MLLMs. The LCS-558K image-text pair dataset is used for the first alignment stage pre-training and only the parameters of the projector are optimized while all the others are frozen. The 665K multi-dataset mixed instruction-following data samples are performed for the second instruction-tuning stage. The projector and LLM are jointly optimized during this stage, while the visual encoder keeps frozen. The batch size of the two stage training is set as 256 and 96, respectively. The AdamW optimizer with a Cosine learning rate schedule is adopted and the initial learning rate is set as 1e-3 and 2e-5 for the two stage training. The models are trained on $8 \times$ NVIDIA A100 40GB GPUs.

4.3 Experimental Results

Multiple groups of multimodal evaluation tasks are performed for comprehensively verifying the effectiveness and capabilities of our SAEP projector.

²<https://github.com/CircleRadon/TokenPacker>

Method	# Tokens	MME POS	MMB SR/OL/PR	SEED SR/IL	VSR test	Avg. ^N
LLaVA-1.5	576	148.3	20.0 / 45.7 / 25.0	51.0 / 59.6	51.5	46.7
Resampler	144	93.3	24.4 / 35.8 / 37.5	44.4 / 51.9	52.4	41.9
C-Abstractor	144	123.3	20.0 / 45.7 / 37.5	48.6 / 57.2	53.5	46.3
LDPv2	144	121.7	20.0 / 46.9 / 25.0	50.8 / 60.1	52.6	45.2
Tokenpacker	144	116.7	17.8 / 39.5 / 45.8	50.5 / 60.9	54.4	46.8
SAEP	144	121.7	24.4 / 46.9 / 58.3	53.3 / 60.9	55.7	51.4

Table 2: Results on the multimodal spatial tasks. “Avg.^N” refers to the normalized average score on the 7 tasks. “MLP” refers to the two-layer MLP projector of LLaVA-1.5¹. The best performance among all the token reduction methods is marked in **bold**.

4.3.1 Performances on Spatial Understanding Tasks

Honeybee adopts 6 tasks to assess the spatial understanding capabilities, including the Position (POS) sub-task of MME, Spatial Relationship (SR), Object Location (OL), and Physical Relation (PR) of MMBench, Spatial Relation (SR) and Instance Location (IL) of SEED-Bench. In addition to the above 6 tasks, the Visual Spatial Reasoning (VSR) task is also included in this group of evaluation tasks.

Table 2 provides the results of the baseline projectors on these 7 spatial understanding tasks. Notably, the SAEP projector demonstrates its advantage on visual spatial understanding with a large average score margin compared to previous SoTA method (51.4 vs. 46.8).

Interestingly, it can also be found that compared to the one-to-one transformed MLP projector, the multi-level visual feature based projectors (i.e., Tokenpacker and SAEP) not only reduce 75% visual tokens but also get better performance. On the contrary, the single-level based token reduction methods (i.e., Resampler, C-Abstractor and LDPv2) underperform the MLP projector on these spatial tasks. This phenomenon further verifies the directly compressing the visual token sequence will disrupt the spatial knowledge implicit in the original sequence and introducing multi-level visual features is a cost-effective choices.

4.3.2 Performances on Visual Location Tasks

The first group of evaluation tasks aims to assess the visual grounding abilities (i.e., locating the object in the given image based on the textual description). Three most popular visual grounding (i.e., Refcoco, Refcoco+ and Refcocog) benchmarks are

adopted.

The evaluation results are provided in Table 3. It can be seen that our SAEP projector shows significant performance improvement on the three visual grounding benchmarks. Compare to the SoTA token reduction method (LDPv2 with 57.4), the proposed SAEP projector gets a large performance margin (+4.0). Moreover, multiple token reduction projectors get better performance than the standard MLP projector, which indicates that the projector not only projects the visual feature to the token embedding space, but also plays an critical role in extracting visual semantics for the LLM backbone. Among them, our SAEP projector performs best and achieves 9.7 absolute accuracy score gain while reducing 75% visual tokens compared to the standard MLP projector (51.7).

When taking the projector architecture into account, the effectiveness of the SAEP projector’s design on modeling the spatial and locational knowledge can be further verified. In specific, although the LDPv2 is the same convolution-based method as the SAEP projector, the SAEP projector further benefits from the leveraging of multi-level features. However, even though the Tokenpacker utilizes the multi-level fine-grained features to enhance the performance, its cross-attention based architecture makes it disadvantaged at extracting the spatial and locational knowledge compared to the convolution-based SAEP projector.

4.3.3 Performances on General Multimodal Task

The third group of tasks includes both the general vision-language tasks (i.e., VQAv2, GQA, Vizwiz and TextVQA) and popular instruction-following MLLM benchmarks (i.e., POPE, MME, MMBench, SEED-Image and MMVet), aiming to evaluate the

Method	#Tokens	Refcoco	Refcoco+	Refcocog	Avg.
		val / testA / testB	val / testA / testB	val / test	
LLaVA-1.5	576	55.2 / 63.1 / 46.4	49.7 / 58.7 / 38.1	51.4 / 50.7	51.7
Resampler	144	31.9 / 34.9 / 28.9	21.0 / 26.3 / 18.0	25.0 / 24.3	26.3
C-Abstractor	144	60.0 / 64.7 / 55.5	50.5 / 58.2 / 44.6	53.3 / 54.7	55.2
LDPv2	144	61.5 / 66.4 / 57.0	54.1 / 62.2 / 46.7	55.6 / 56.9	57.6
Tokenpacker	144	60.6 / 65.9 / 56.8	53.1 / 61.4 / 46.8	55.9 / 56.9	57.2
SAEP	144	65.5 / 67.6 / 63.4	58.3 / 63.5 / 52.9	59.8 / 60.3	61.4

Table 3: Accuracy results of the SAEP projector and the baselines on the visual grounding tasks. The Accuracy is calculated based the Intersection Over Union (IOU) ratio between the predicted and actual bounding boxes, with an IOU exceeding 0.5 classified as a true positive.

Method	#Token	VQAv2	GQA	Vizwiz	VQA ^T	POPE	MME	MMB	SEED	MMVet
LLaVA-1.5	576	78.5	62.0	50.0	58.2	85.9	1511/297	64.3	58.6	31.1
Resampler	144	73.3	56.6	50.2	52.4	83.6	1348/259	63.1	58.0	26.0
C-Abstractor	144	76.5	59.9	51.1	56.2	84.6	1471/293	65.0	62.4	29.8
LDPv2	144	77.8	60.7	50.0	<u>57.1</u>	84.9	1446/267	66.4	<u>65.2</u>	28.0
TokenPacker	144	<u>78.1</u>	<u>61.1</u>	<u>52.0</u>	58.0	85.9	1432/277	65.7	64.9	32.8
SAEP	144	78.5	62.4	53.0	58.0	85.9	<u>1467/316</u>	<u>66.3</u>	65.4	<u>30.6</u>

Table 4: Results on general multimodal tasks. The best performance on each task is marked with **bold** and the second-best is marked with underlined. The MME benchmark includes two sub-tasks: perception and cognition.

general vision-language understanding capabilities.

The results are shown in Table 4. Compared to the baselines, the SAEP projector gets best performance on 5 of 10 tasks and gets second-best on another 5 tasks. That indicates that the SAEP projector has the ability to preserve sufficient global visual semantic information for the MLLM while significantly reducing the number of visual token.

Overall, the results in Table 4 shows that as a token reduction projector, the computational efficiency brought by the SAEP projector does not come at the cost of the multimodal understanding and reasoning abilities of the MLLM. More than that, the performance shown in Table 2 and Table 3 can further proven the superiority of the SAEP projector on extracting and restructuring visual spatial and locational knowledge.

5 Ablation Study

5.1 Efficiency Improvement

To illustrate the efficiency improvement brought by our SAEP, the comparisons from multiple perspectives between the original MLP projector and our SAEP projector are provided in Table 5. Moreover, the efficiency of the SAEP projector with 64 visual tokens is also employed and evaluated. The performance difference are shown in Figure 1 (a). To be

Method	#Tokens	TPS	PT	IT
MLP	576	29.1	3.5h	10h
SAEP	144	34.2	1h	7.8h
SAEP	64	35.2	0.6h	7.4h

Table 5: Training times with 8 NVIDIA A100 40GB GPUs and same LLaVA training recipe. “PT” and “IT” is the abbreviation of “Pre-training” and “Instruction-tuning”. “TPS” refers to “token per second”.

clear, the token per second (TPS) is evaluated on the MMVet test set by One A100 GPU.

Table 5 indicates that our SAEP projector with 144 token can save about 35% training time compared to the MLP projector, while the SAEP projector with 64 token can further save 40.7%. In addition, the results on TPS show that the 144-token and 64-token SAEP projectors boost the inference efficiency by 17.5% and 21.0% respectively. Meanwhile, as illustrated in Figure 1 (a), even though the visual token is reduced by 89%, the SAEP projector is still able to perform better than the MLP projector on the spatial and locational tasks, and the performance on the general multimodal tasks is comparable. Therefore, our SAEP projector can not only significantly improve the computational efficiency, but also enhance the spatial and locational

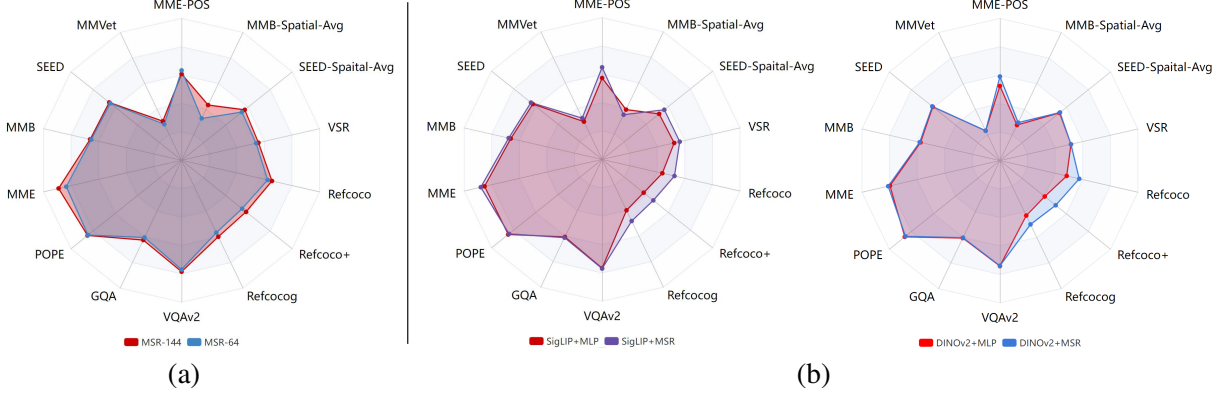


Figure 1: (a) The performance of the SAEP projector with different number of visual tokens. (b) The performance of the MLP and our SAEP projector with different visual encoders. “MMB-Spatial-Avg” and “SEED-Spatial-Avg” are the average score of MMB and SEED’s spatial sub-tasks.

capabilities of the MLLM.

5.2 Effectiveness on Other Visual Encoder

As a token reduction projector, the generalization ability of the proposed SAEP on different visual encoder is very important. Besides to the adopted CLIP-ViT visual encoder, another two popular visual encoders, SigLIP and DINOv2, are select to verify the SAEP projector’s generalization. The training recipe is the same as the LLaVA-1.5 except for the visual encoder. The input image size of both the SigLIP and DINOv2 is 224px. The results are shown in Figure 1. It is obvious that with the two different visual encoders, the efficient SAEP projector still demonstrate its advantage on enhancing the spatial and locational abilities of the MLLM. It can also be seen that the SAEP projector can get slight performance improvement on the general multimodal tasks. In a word, the SAEP is an general spatial and locality-enhanced efficient projector.

5.3 Architecture Design Ablation

There are three main components adopted in the SAEP projector: point-wise convolution with multi-level visual features, a depth-wise convolution layer and an average pooling layer. We conduct a group of ablation studies to verify the effectiveness of the SAEP’s design and the results are provided in Table 6.

It can be seen that removing each component will result in a decrease in performance, which indicate that all the three components are helpful to the final performance improvement. Besides, it can be also found that introducing multi-level visual features makes the greatest contribution to the final

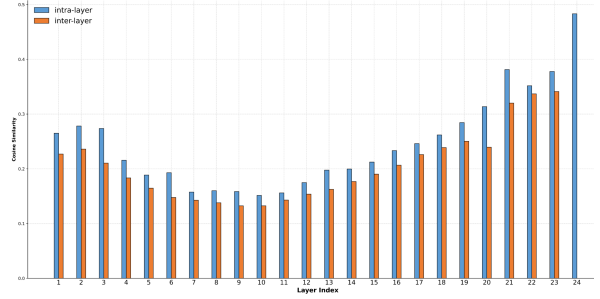


Figure 2: Average cosine similarity over 300 images calculated by the CLIP intra-layer and inter-layer. Inter-layer means the layer X and its adjacent layer $X + 1$.

performance. That denotes that providing supplementary detailed local information is beneficial to improve the visual understanding and reasoning abilities, especially for the token reduction projector. Meanwhile, the results also reveal that the “residual” connection between the depth-wise convolution operation and average pooling operation mainly contributes to capture the spatial and locational information.

5.4 Exploration on the Layer Selection Strategy

The SAEP projector utilizes the multi-level visual features to supplementary fine-grained local information. Even though some recent MLLM works (e.g. TokenPacker) have realized that introducing multi-level visual features is beneficial for the performance, there is no an available explicit guideline to select the most suitable visual features from different layers. All these works have to select the features from different layers by experience and iterative testing.

We propose a novel layer selection strategy and

Multi-level	Conv.	Pooling	S-Avg.	L-Avg.	GQA	VQA ^T	POPE	MMB	SEED
✓	✓	✓	51.4	61.4	62.4	58.0	85.0	66.3	65.4
✓	×	✓	47.9 (-3.5)	61.4	61.9	57.6	84.6	66.2	65.3
✓	✓	×	46.8 (-4.6)	58.7 (-2.7)	61.1	57.8	84.9	66.0	64.9
×	✓	✓	44.7 (-6.7)	57.6 (-3.8)	61.2	56.8	64.8	65.6	64.6

Table 6: Component-wise ablation results of the proposed SAEP projector. “S-Avg.” and “L-Avg.” refers to the average score of the above adopted visual spatial and location tasks respectively.

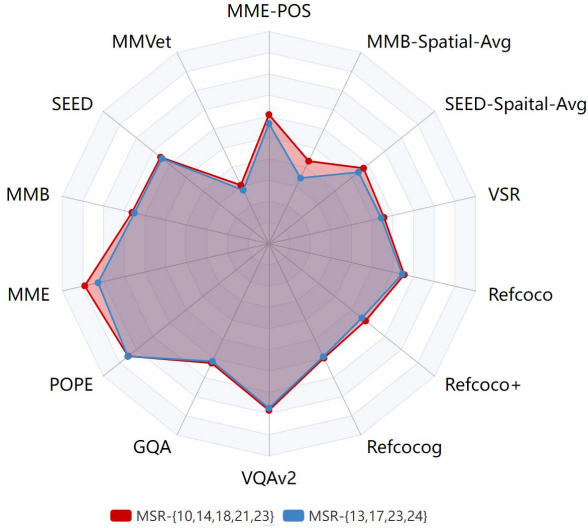


Figure 3: Average cosine similarity over 300 images calculated by the CLIP intra-layer and inter-layer. Inter-layer means the layer X and its adjacent layer $X + 1$.

verify its effectiveness by a fair comparison. We firstly estimate the cosine similarity of inter- and intra-layer visual features of CLIP on 100 images. The average similarity scores of different layers are visualized in Figure 2. The most obvious characteristic is that as the number of layers increases, the intra-layer and inter-layer similarity both first decreases and then increases. The forward propagation of CLIP is a process where the visual information gradually becomes more concrete and then more abstract. In other words, as the number of layers increases, the model first gets a accurate understanding of each path-level local visual feature. Then, with the layer number increases, the model begins to aggregate the local detailed information and capture more abstract, global information. This is also consistent with the viewpoint of recent research (Jiang et al., 2023b). Therefore, the 10th layer is selected because its intra-layer similarity is the lowest.

Meanwhile, an anomalous layer can be observed in Figure 2. The 21st layer exhibits high intra-

layer similarity, low similarity with the 20th layer, but high similarity with the 22nd layer. This indicates that this layer is the information pivot and it captures the most generalized global information, the visual features captured by the deeper layer are more optimization-specific. Thus, the 21st layer is selected. Additionally, our evaluation shows that the similarity decreases as the layer distance increases. Consequently, we uniformly sample the 14th and 18th layers between the 10th and 21st layers, and include the commonly used 23rd layer, forming the set of all selected layers.

To verify the effectiveness of the above layer selection strategy, we make a fair comparison between the set of $\{10,14,18,21,23\}$ layers with the set of $\{13,17,23,24\}$ layers, the former layer set is adopted by the TokenPacker and gets best performance among multiple layer sets. The comparison results are shown in Figure 3, our layer selection method get better performance. In fact, the ablation experiment conducted in Section 5.2, which applies the SAEP projector on the DINOv2 and SigLIP model, is also guided by the above layer selection strategy and obtains significant performance improvement as shown in Figure 5.2. These results not only demonstrate the performance gain brought by an optimal layer sets, but also highlight the worth of our layer selection strategy.

6 Conclusion

Despite the crucial role played by the projector in multi-modal language models (MLLMs), its in-depth analysis and exploration remain limited. To address the issue of spatial information discrepancy between 2D visual token sequences and textual token sequences, we propose a spatially aware efficient projector (SAEP) based on multi-layer visual features. Experimental results demonstrate that our SAEP not only significantly reduces the number of visual tokens, thereby substantially improving the training and inference efficiency of MLLMs,

but also significantly enhances the MLLM’s ability to understand spatial information. Furthermore, our SAEP exhibits strong performance on the most popular multi-modal evaluation benchmarks compared to existing projectors. Further analysis not only highlights the strong compatibility of SAEP with other visual encoders but also validates the effectiveness of our architectural design.

References

- Josh Achiam, Steven Adler, Sandhini Agarwal, Lama Ahmad, Ilge Akkaya, Florencia Leoni Aleman, Diogo Almeida, Janko Altschmidt, Sam Altman, Shyamal Anadkat, et al. 2023. Gpt-4 technical report. *arXiv preprint arXiv:2303.08774*.
- Jean-Baptiste Alayrac, Jeff Donahue, Pauline Luc, Antoine Miech, Iain Barr, Yana Hasson, Karel Lenc, Arthur Mensch, Katherine Millican, Malcolm Reynolds, et al. 2022. Flamingo: a visual language model for few-shot learning. *Advances in neural information processing systems*, 35:23716–23736.
- Yutong Bai, Xinyang Geng, Karttikeya Mangalam, Amir Bar, Alan L Yuille, Trevor Darrell, Jitendra Malik, and Alexei A Efros. 2024. Sequential modeling enables scalable learning for large vision models. In *Proceedings of the IEEE/CVF Conference on Computer Vision and Pattern Recognition*, pages 22861–22872.
- Mu Cai, Jianwei Yang, Jianfeng Gao, and Yong Jae Lee. 2024. Matryoshka multimodal models. *arXiv preprint arXiv:2405.17430*.
- Junbum Cha, Wooyoung Kang, Jonghwan Mun, and Byungseok Roh. 2024. Honeybee: Locality-enhanced projector for multimodal llm. In *Proceedings of the IEEE/CVF Conference on Computer Vision and Pattern Recognition*, pages 13817–13827.
- Xi Chen, Xiao Wang, Soravit Changpinyo, AJ Piergiovanni, Piotr Padlewski, Daniel Salz, Sebastian Goodman, Adam Grycner, Basil Mustafa, Lucas Beyer, et al. 2022. Pali: A jointly-scaled multilingual language-image model. In *The Eleventh International Conference on Learning Representations*.
- Wei-Lin Chiang, Zhuohan Li, Zi Lin, Ying Sheng, Zhanghao Wu, Hao Zhang, Lianmin Zheng, Siyuan Zhuang, Yonghao Zhuang, Joseph E. Gonzalez, Ion Stoica, and Eric P. Xing. 2023. Vicuna: An open-source chatbot impressing gpt-4 with 90%* chatgpt quality.
- Xiangxiang Chu, Limeng Qiao, Xinyu Zhang, Shuang Xu, Fei Wei, Yang Yang, Xiaofei Sun, Yiming Hu, Xinyang Lin, Bo Zhang, et al. 2024a. Mobilevlm v2: Faster and stronger baseline for vision language model. *arXiv preprint arXiv:2402.03766*.
- Xiangxiang Chu, Limeng Qiao, Xinyu Zhang, Shuang Xu, Fei Wei, Yang Yang, Xiaofei Sun, Yiming Hu, Xinyang Lin, Bo Zhang, et al. 2024b. Mobilevlm v2: Faster and stronger baseline for vision language model. *arXiv preprint arXiv:2402.03766*.
- Xiaoyi Dong, Pan Zhang, Yuhang Zang, Yuhang Cao, Bin Wang, Linke Ouyang, Xilin Wei, Songyang Zhang, Haodong Duan, Maosong Cao, et al. 2024a. Internlm-xcomposer2: Mastering free-form text-image composition and comprehension in vision-language large model. *arXiv preprint arXiv:2401.16420*.
- Xiaoyi Dong, Pan Zhang, Yuhang Zang, Yuhang Cao, Bin Wang, Linke Ouyang, Songyang Zhang, Haodong Duan, Wenwei Zhang, Yining Li, et al. 2024b. Internlm-xcomposer2-4khd: A pioneering large vision-language model handling resolutions from 336 pixels to 4k hd. *arXiv preprint arXiv:2404.06512*.
- Alexey Dosovitskiy. 2020. An image is worth 16x16 words: Transformers for image recognition at scale. *arXiv preprint arXiv:2010.11929*.
- Peng Gao, Renrui Zhang, Chris Liu, Longtian Qiu, Siyuan Huang, Weifeng Lin, Shitian Zhao, Shijie Geng, Ziyi Lin, Peng Jin, et al. 2024. Sphinx-x: Scaling data and parameters for a family of multi-modal large language models. *CoRR*.
- Andrew Jaegle, Felix Gimeno, Andy Brock, Oriol Vinyals, Andrew Zisserman, and Joao Carreira. 2021. Perceiver: General perception with iterative attention. In *International conference on machine learning*, pages 4651–4664. PMLR.
- Albert Q Jiang, Alexandre Sablayrolles, Antoine Roux, Arthur Mensch, Blanche Savary, Chris Bamford, Devendra Singh Chaplot, Diego de las Casas, Emma Bou Hanna, Florian Bressand, et al. 2024. Mixtral of experts. *arXiv preprint arXiv:2401.04088*.
- Dongsheng Jiang, Yuchen Liu, Songlin Liu, Xiaopeng Zhang, Jin Li, Hongkai Xiong, and Qi Tian. 2023a. From clip to dino: Visual encoders shout in multi-modal large language models.
- Dongsheng Jiang, Yuchen Liu, Songlin Liu, Xiaopeng Zhang, Jin Li, Hongkai Xiong, and Qi Tian. 2023b. From clip to dino: Visual encoders shout in multi-modal large language models.
- Siddharth Karamcheti, Suraj Nair, Ashwin Balakrishna, Percy Liang, Thomas Kollar, and Dorsa Sadigh. 2024. Prismatic vlms: Investigating the design space of visually-conditioned language models. In *Forty-first International Conference on Machine Learning*.
- Bo Li, Peiyuan Zhang, Jingkan Yang, Yuanhan Zhang, Fanyi Pu, and Ziwei Liu. 2023a. Otterhd: A high-resolution multi-modality model. *arXiv preprint arXiv:2311.04219*.

- Feng Li, Renrui Zhang, Hao Zhang, Yuanhan Zhang, Bo Li, Wei Li, Zejun Ma, and Chunyuan Li. 2024a. Llava-next-interleave: Tackling multi-image, video, and 3d in large multimodal models. *arXiv preprint arXiv:2407.07895*.
- Junnan Li, Dongxu Li, Silvio Savarese, and Steven Hoi. 2023b. Blip-2: Bootstrapping language-image pre-training with frozen image encoders and large language models. *arXiv preprint arXiv:2301.12597*.
- Wentong Li, Yuqian Yuan, Jian Liu, Dongqi Tang, Song Wang, Jianke Zhu, and Lei Zhang. 2024b. Token-packer: Efficient visual projector for multimodal llm. *arXiv preprint arXiv:2407.02392*.
- Yanhao Li, Hanzi Mao, Ross Girshick, and Kaiming He. 2022. Exploring plain vision transformer backbones for object detection. In *European conference on computer vision*, pages 280–296. Springer.
- Yanwei Li, Yuechen Zhang, Chengyao Wang, Zhisheng Zhong, Yixin Chen, Ruihang Chu, Shaoteng Liu, and Jiaya Jia. 2024c. Mini-gemini: Mining the potential of multi-modality vision language models. *arXiv preprint arXiv:2403.18814*.
- Zhang Li, Biao Yang, Qiang Liu, Zhiyin Ma, Shuo Zhang, Jingxu Yang, Yabo Sun, Yuliang Liu, and Xiang Bai. 2024d. Monkey: Image resolution and text label are important things for large multi-modal models. In *Proceedings of the IEEE/CVF Conference on Computer Vision and Pattern Recognition*, pages 26763–26773.
- Haotian Liu, Chunyuan Li, Yuheng Li, and Yong Jae Lee. 2023a. Improved baselines with visual instruction tuning.
- Haotian Liu, Chunyuan Li, Yuheng Li, Bo Li, Yuanhan Zhang, Sheng Shen, and Yong Jae Lee. 2024. Llava-next: Improved reasoning, ocr, and world knowledge.
- Haotian Liu, Chunyuan Li, Qingyang Wu, and Yong Jae Lee. 2023b. Visual instruction tuning. In *NeurIPS*.
- Maxime Oquab, Timothée Darcet, Théo Moutakanni, Huy V Vo, Marc Szafraniec, Vasil Khalidov, Pierre Fernandez, Daniel HAZIZA, Francisco Massa, Alaaeldin El-Nouby, et al. Dinov2: Learning robust visual features without supervision. *Transactions on Machine Learning Research*.
- Alec Radford, Jong Wook Kim, Chris Hallacy, Aditya Ramesh, Gabriel Goh, Sandhini Agarwal, Girish Sastry, Amanda Askell, Pamela Mishkin, Jack Clark, et al. 2021. Learning transferable visual models from natural language supervision. In *International conference on machine learning*, pages 8748–8763. PMLR.
- Yuzhang Shang, Mu Cai, Bingxin Xu, Yong Jae Lee, and Yan Yan. 2024. Llava-prumerge: Adaptive token reduction for efficient large multimodal models. *arXiv preprint arXiv:2403.15388*.
- Chameleon Team. 2024. Chameleon: Mixed-modal early-fusion foundation models. *arXiv preprint arXiv:2405.09818*.
- Hugo Touvron, Louis Martin, Kevin Stone, Peter Albert, Amjad Almahairi, Yasmine Babaei, Nikolay Bashlykov, Soumya Batra, Prajjwal Bhargava, Shruti Bhosale, et al. 2023. Llama 2: Open foundation and fine-tuned chat models. *arXiv preprint arXiv:2307.09288*.
- An Yang, Baosong Yang, Binyuan Hui, Bo Zheng, Bowen Yu, Chang Zhou, Chengpeng Li, Chengyuan Li, Dayiheng Liu, Fei Huang, et al. 2024. Qwen2 technical report. *arXiv preprint arXiv:2407.10671*.
- Xiaohua Zhai, Basil Mustafa, Alexander Kolesnikov, and Lucas Beyer. 2023. Sigmoid loss for language image pre-training. In *Proceedings of the IEEE/CVF International Conference on Computer Vision*, pages 11975–11986.
- Pan Zhang, Xiaoyi Dong Bin Wang, Yuhang Cao, Chao Xu, Linke Ouyang, Zhiyuan Zhao, Shuangrui Ding, Songyang Zhang, Haodong Duan, Hang Yan, et al. 2023. Internlm-xcomposer: A vision-language large model for advanced text-image comprehension and composition. *arXiv preprint arXiv:2309.15112*.